Experimental and Theoretical Investigation of the Effect of Lubricant Structure on the Bonding Kinetics of Perfluoroalkylpolyethers on CH_x Amorphous Hydrogenated Carbon

R. J. Waltman

IBM Storage Systems, 5600 Cottle Road, San Jose, California 95193

Received February 17, 2000. Revised Manuscript Received May 9, 2000

Perfluoropolyethers (PFPEs) are widely used as topical lubricants on rigid magnetic media to provide a low wear interface. The tribological reliability of the disk storage device is strongly dependent upon the mobile state of the lubricant. In this work, the kinetics of the bonding of molecularly thin (11 Å) Demnum-OH films to the CH_x amorphous, hydrogenated carbon overcoat is investigated. Demnum-OH has the chemical structure $F(CF_2CF_2CF_2O)_n$-$CF_2CF_2CH_2OH$, compared to the more widely used Zdol PFPE lubricant having the $-(CF_2$-$CF_2O)-///-(CF_2O)-$ backbone capped by $-CH_2OH$ hydroxyl groups on both ends of the molecule. The focal point of these studies is to investigate how differences in the PFPE chemical structure, in particular the backbone, affect both the flexibility of the lubricant chain and their interactions with the carbon surface. The bonding rate of Demnum-OH on CH_x is investigated by recording the changes in the infrared sprectrum of Demnum-OH as a function of time, temperature, and molecular weight. The bonding kinetics are described by a differential rate equation that has a time dependent rate coefficient, $k(t) = k_0t^{-h}$. The functional form of the time dependence in the bonding kinetics is interpreted to reflect the ability of the lubricant to adopt configurations compatible with bonding. The kinetic results for the Demnum-OH bonding, $k(t) \alpha t^{-0.5}$, indicate a stiff chain compared to Zdol, where $k(t) \alpha t^{-1.0}$. The differences in the observed time dependence are related to the chemical structure of the monomer units and the energetic barriers to internal rotation about the C−O and C−C bonds (via ab initio, molecular mechanics calculations). These results suggest significant confinement of the Demnum chain consistent with a more solidlike adsorbed film structure compared to flexible (high C1:C2 ratio) Zdol.

Introduction

The behavior and properties of molecularly thin liquid films of several monolayers or less supported by surfaces have received considerable attention not only because of their technological importance, e.g., in boundary lubrication, but also because of their considerable departure from bulk behavior. For example, molecularly thin organic films on surfaces exhibit diffusion coefficients that are thickness dependent and show unusual flow profiles on surfaces that is a result of molecular alignment or ordering.[1] In turn, molecular alignment can cause the confinement of molecular films in the boundary layer, giving rise to solidlike and liquidlike behavior.[2,3] The confinement may additionally affect boundary layer mobility, by inducing a dimensional or geometric dependence in the diffusion-limited random walk, resulting in anamolous time dependences of the rate constants.[4,5] Thus, the physics required to provide a description of the behavior of molecularly thin films on surfaces are often not scalable to, and can depart considerably from, their bulk counterparts.

Monomolecular perfluoropolyether (PFPE) films, such as the Fomblin Zdol or Demnum-OH, provide wear protection by serving as topical lubricants on the amorphous carbon overcoats of rigid magnetic media, or computer disks. However, recent studies on these systems have revealed that PFPE lubricants also exhibit

(1) Cazabat, A. M. *C. R. Acad. Sci.* **1990**, *310*, 107. Cazabat, A. M.; Fraysse, N.; Heslot, F.; Carles, P. *J. Phys. Chem.* **1990**, *94*, 7581. Cazabat, A. M.; Valignat, M. P.; Villette, S.; DeConinck, J.; Louche, F. *Langmuir* **1997**, *13*, 4754.

(2) Demirel, A. L.; Granick, S. *Phys. Rev. Lett.* **1996**, *77*, 2261. Granick, S. *Science* **1991**, *253*, 1374. Klein, J.; Kumacheva, E. *J. Chem. Phys.* **1998**, *108*, 6996. Kumacheva, E.; Klein, J. *J. Chem. Phys.* **1998**, *108*, 7010. Yoshizawa, H.; Israelachvili, J. *J. Phys. Chem.* **1993**, *97*, 11300. Israelachvili, J. N.; Chen, Y.-L.; Yoshizawa, H. *J. Adhes. Sci. Technol.* **1994**, *8*, 1231.

(3) Wallace, W. E.; van Zanten, J. H.; Wu, W.-L. *Phys. Rev. E* **1995**, *52*, 3329. van Zanten, J. H.; Wallace, W. E.; Wu, W.-L. *Phys. Rev. E* **1996**, *53*, 2053. Keddie, J. L.; Jones, R. A. L.; Cory, R. A. *Faraday Discuss.* **1994**, *98*, 219. Forrest, J. A.; Svanberg, C.; Révész, K.; Rdahl, M.; Torell, L. M.; Kasemo, B. *Phys. Rev. E* **1998**, *58*, 1226. Forrest, J. A.; Dalnoki-Veress, K.; Stevens, J. R.; Dutcher, J. R. *Phys. Rev. Lett.* **1996**, *77*, 2002. Mansfield, K. F.; Theodorou, D. N. *Macromolecules* **1991**, *24*, 6283. Satomi, N.; Takahara, A.; Kajiyama, T. *Macromolecules* **1999**, *32*, 4474. Kajiyama, T.; Tanaka, K.; Takahara, A. *Macromolecules* **1997**, *30*, 280. Tanaka, K.; Taura, A.; Ge, S.-R.; Takahara, A.; Kajiyama, T. *Macromolecules* **1996**, *29*, 3040.

(4) Kopelman, R. In *The Fractal Approach to Heterogeneous Chemistry*, Avnir, D., Ed.; John Wiley & Sons Ltd.: Chichester, U.K., 1989; pp 295−309. Kopelman, R. *Science* **1988**, *241*, 1620. Argyrakis, P.; Kopelman, R. *J. Phys. Chem.* **1989**, *93*, 225. Argyrakis, P.; Kopelman, R.; Lindenberg, K. *Chem. Phys.* **1993**, *177*, 693. Lindenberg, K.; Argyrakis, P.; Kopelman, R. *J. Phys. Chem.* **1995**, *99*, 7542.

(5) Ovchinnikov, A. A.; Zeldovich, Y. B. *Chem. Phys.* **1978**, *28*, 215.

10.1021/cm0001410 CCC: $19.00
Published on Web 06/23/2000

many of the properties of monomolecular films on surfaces described above. In the thickness regime typically employed for these materials, ~10−30 Å, the physical and chemical properties of these "liquid" lubricants, and hence their resulting tribological performance,[6] are intimately coupled to the interactions that occur at the lubricant−carbon interface.[7−10]

Recent work by Waltman et al.[10] on the bonding kinetics of monomolecular Zdols on amorphous hydrogenated carbon (CH_x) indicated a considerable dependence on the Zdol main chain structure. The bonding kinetics were described by a differential rate equation that had a time dependent rate coefficient, $k(t) = k_o t^{-h}$. By varying the ratio of the perfluoromethylene oxide (C1) to perfluoroethylene oxide (C2) monomer units, the exponent h in the time dependence was observed to vary from 0.5 (low C1:C2 ratio) to 1.0 (high C1:C2 ratio). The lower C1:C2 ratio produced bonding from a more solidlike adsorbed film, while the higher C1:C2 ratio produced bonding from a more liquidlike adsorbed film. The functional form of the time dependence in the bonding kinetics was interpreted to reflect the ability of the lubricant to adopt configurations compatible with bonding, consistent with surface energy data.[9,11] The variation of the Zdol chain flexibility on the bonding kinetics was interpreted on the basis of the energetic barriers to internal rotation. The influence of chain flexibility in the adsorption of macromolecules onto surfaces is well-established.[12,13] In PFPEs, the effect of molecular structure (C1:C2 ratio) was observed to impact the bulk T_g in an analogous manner.[14] Surface T_g's of molecularly thin polymer films supported by substrates are also impacted by the high surface area-to-volume ratio. For a strongly interacting polymer−surface, confinement effects can dominate and generally cause an increase in the T_g of the adsorbed film, while, for a noninteracting polymer−surface, a reduction in the T_g of the adsorbed film is generally observed.[3] What is actually observed is therefore strongly dependent upon which effect is dominant, i.e., polymer−surface intermolecular interactions, internal property of the adsorbed film such as chain flexibility, or external parameter such as temperature. Finally, NMR studies of PFPE lubricants have shown evidence for polymer−substrate interactions with decreasing film thickness.[15]

In this report, we continue our studies on the influence of chain flexibility and bonding kinetics of perfluoroether lubricants, as lubricant bonding is a significant determinant of tribological reliability.[16] The focal point of these studies is the determination of the functional form of the time dependence in the bonding of Demnum-OH lubricants to the CH_x amorphous hydrogenated carbon surface. Demnum differs from Zdol as it is essentially a homopolymer composed of perfluoropropylene oxide monomer units.

$$HO-CH_2CF_2O-[CF_2O]_x-[CF_2CF_2O]_y-CF_2CH_2-OH \quad \text{Zdol}$$

$$F-[CF_2CF_2CF_2O]_y-CF_2CF_2CH_2-OH \quad \text{Demnum-OH}$$

Since the glass transition temperature, T_g, of *bulk* Demum-OH is ~40−50 °C greater than for Zdol,[14] the chain stiffness is expected to be greater. Thus, the influence of the chain flexibility is additionally investigated by ab initio and molecular mechanics computational modeling techniques to provide insight into the observed kinetics and the role of lubricant chain flexibility/mobility in bonding.

Experimental Section

Materials. The carbon substrates used in these studies were 65 mm diameter computer hard disks composed of a supersmooth glass substrate (root mean square roughness of ~10 Å) onto which were sputter-deposited an underlayer of Cr, a Cobalt-based magnetic layer, and nominally ~100 Å of CH_x. The atomic composition of the CH_x surfaces has been quantified previously.[9] The perfluoropolyether fluids used in this work were obtained from Daikin under the trade name Demnum-SA and from Ausimont under the trade name Zdol. The Demnum samples used in these studies were SA1, SA2, and SA3 with molecular weights of 2200, 3000, and 5500, respectively.

Kinetics Measurements. The lubricants were applied to the disks from solvents using the dip-coat method. For the kinetics studies, all disks were coated with an initial film thickness of 11.0 ± 0.5 Å. After lubricant application, the disks were placed into ovens and annealed in air at 64, 90, 120, and 150 °C. The humidity in the ovens was measured to be 4% at 64 °C, <2% at 90 °C, and <1% at 120 and 150 °C. The changes in the mobile and bonded quantities of lubricant were measured as a function of time at each of the annealing temperatures. Throughout the following, we refer to the lubricant on the disk surface as being either "bonded" or "mobile". The lubricant retained by the disk following the solvent extraction is defined as the amount bonded, while that removed is defined as the mobile lubricant.[9] We note that our use of the term bonded lubricant follows the convention historically utilized in the data storage community to describe that fraction of lubricant more tightly adhered to the carbon surface, but it does not necessarily imply chemisorption.

Infrared Data. The bonding and evaporation kinetics of Demnum-OH were measured by following the changes in the infrared spectrum as a function of time. For these purposes, a Nicolet Model 560 FTIR was employed. The lubricant thickness was calibrated to the absorbance of the 1250 cm^{-1} band maximum (in reflectance) by ellipsometry. It is imperative to understand the infrared spectrum of Demnum to provide a basis for interpretation of the IR results. We therefore provide a brief description of the infrared spectrum of Demnum, poly(perfluoro-*n*-propylene oxide), or $-[CF_2CF_2CF_2O]_n-$, using $CF_3O[CF_2CF_2CF_2O]CF_3$ (PFNPO) as our computationally tractable, structural model. Molecular orbital calculations on

(6) Wang, R.-H.; White, R. L.; Meeks, S. W.; Min, B. G.; Kellock, A.; Homola, A.; Yoon, D. *IEEE Trans. Magn.* **1996**, *32*, 3777. Karis, T.; Tyndall, G. W.; Waltman, R. J. *Tribol. Lett.* submitted for publication. Kim, H. I.; Mate, C. M.; Hannibal, K. A.; Perry, S. S. *Phys. Rev. Lett.* **1999**, *82*, 3496.

(7) Waltman, R. J.; Tyndall, G. W.; Pacansky, J. *Langmuir* **1999**, *15*, 6470.

(8) Tyndall, G. W.; Waltman, R. J.; Pocker, D. *Langmuir* **1998**, *14*, 7527.

(9) Waltman, R. J.; Pocker, D.; Tyndall, G. W. *Tribol. Lett.* **1998**, *4*, 267.

(10) Waltman, R. J.; Tyndall, G. W.; Pacansky, J.; Berry, R. J. *Tribol. Lett.* **1999**, *7*, 91.

(11) Tyndall, G. W.; Leezenberg, P. B.; Waltman, R. J.; Castenada, J. *Trib. Lett.* **1998**, *4*, 103.

(12) Silberberg, A. *J. Chem. Phys.* **1967**, *46*, 1105. Silberberg, A. *J. Phys. Chem.* **1962**, *66*, 1872. Silberberg, A. *J. Phys. Chem.* **1962**, *66*, 1884.

(13) Hoeve, C. A.; DiMarzio, E. A.; Peyser, P. *J. Chem. Phys.* **1965**, *42*, 2558.

(14) Marchionni, G.; Ajroldi, G.; Righetti, M. C.;d Pezzin, G. *Macromolecules* **1993**, *26*, 1751.

(15) Yanagisawa, M. *Tribol. Trans.* **1994**, *37*, 629.

(16) Khurshudov, A.; Baumgart, P.; Waltman, R. J. *Wear* **1999**, *225−229*, 690.

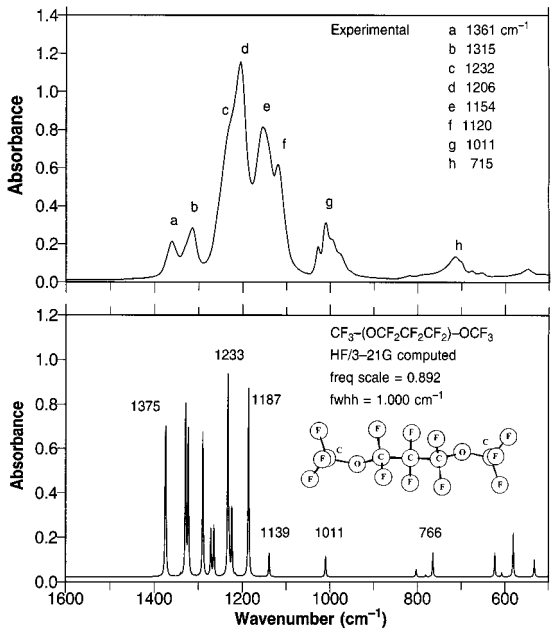

Figure 1. Experimental transmission (top) and SCF/3-21G computed (bottom) infrared spectra for Demnum S-100 (MW $\sim$ 5600) and the $CF_3OCF_2CF_2CF_2OCF_3$ model, respectively. The computed frequency is uniformly scaled by 0.892. The SCF/3-21G optimized geometery for $CF_3OCF_2CF_2CF_2OCF_3$ is shown in the bottom figure. The total energy is −1524.075 544 hartrees.

PFNPO were performed at the SCF/3-21G level of theory using the Gaussian computer program.[17] The 3-21G basis set[18] has been shown to qualititatively reproduce the experimental infrared spectrum of perfluorinated ethers.[19] The harmonic vibrational frequencies were determined by analytic differentiation of the SCF wave function at the optimized geometry; no imaginary frequencies were computed. The experimental transmission (Demnum S-100, MW $\sim$ 5600) and calculated (PFNPO) infrared spectra are presented in Figure 1. The computed vibrational frequencies and their assignment are reproduced in Table 1. The assignments for the infrared bands are based upon normal mode displacement vectors and potential energy distributions (PED[20]), where the latter furnishes the contribution of each force constant to the normal frequencies of vibration. The computed spectrum was simulated using a Lorentzian function for each band, and the bandwidths at half-height were all set equal to 1 cm^{-1}. This procedure is intended for qualitative interpretation and for matching the computed with the observed spectrum as closely as possible. In contrast, the many coupled oscillators in the polymer give rise to rather broad bands observed in the experimental spectrum. A comparison of the infrared spectra indicate good agreement in the positions of the vibrational frequencies. In PFNPO, the relative intensities of the high-frequency vibrations at 1375, 1329, and 1323 cm^{-1} in the computed spectrum are greater than the experimental bands labeled a and b in Figure 1 (top) and are readily explained. These bands are attributed to the C−F stretching modes of the perfluoromethyl end groups which contribute to a greater proportion in the smaller monomer model compared to the much larger polymer. The bands labeled c and d in the experimental spectrum correspond to the computed set of bands 1273 and 1265 cm^{-1} and 1233 cm^{-1}, respectively. They are the combination of C−F stretching vibrations in the CF_2 perfluoromethylene and the C−O stretches in the ether groups. The intense experimental band labeled e is attributed primarily to the C−O ether stretch, corresponding to the 1187 cm^{-1} computed band. The experimental band f corresponds to the computed 1139 cm^{-1} band, largely C−F stretching vibrations of the CF_2 groups. The g and h bands contain the bending modes involving the monomer unit CF_2 and O−C−F structural moieties, Table 1.

Titration Experiments. The maximum quantity of lubricant that can be bonded to the carbon film on the computer disk, i.e., the "titrated" thickness, is determined as a function of molecular weight. An excess thickness of lubricant is applied to the disk and annealed. During the course of the annealing, the bonded quantity is measured (IR) as a function of time until a limiting bonded thickness is attained. The limiting thickness defines the maximum quantity of lubricant that can be physisorbed to the carbon overcoat surface. The bonding kinetics studies are conducted on film thicknesses not exceeding the titrated thickness, which is molecular weight dependent, to ensure adequate surface bonding sites. The results of these titration experiments are shown in Figure 2, where the quantity of titrated Demnum-OH is presented as a function of lubricant molecular weight (MW) and compared to Zdol. For Demnum-OH on CH_x, approximately 17, 23, and 44 Å are maximally bonded for MW = 2200, 3000, and 5500, respectively, while, for Zdol on CH_x, we find that approximately 7, 14, and 25 Å can be maximally bonded with Zdol 1100, 2000, and 4000, respectively. Thus, the slope for the Demnum-OH titration plot is greater than that for the corresponding Zdol, and its significance will be discussed below. For the kinetic experiments reported here, the CH_x surface will not limit the bonding of the initial 11 Å films of the Demnum-OH samples.

Results and Discussion

Kinetic Data. The results of the bonding and evaporation kinetic experiments conducted with Demnum-OH, of MW 2200 and 3000, on amorphous hydrogenated carbon, CH_x, are shown in Figures 3 and 4 as a function of time and temperature between 64 and 150 °C. The rate equations used to obtain a theoretical fit to the observed kinetic data have been developed previously[10] and are show as the solid lines in Figures 3 and 4. The differential rate equations for the formation of bonded lubricant, B, and the evaporation of mobile lubricant, C, both originating from the mobile lubricant, A, may be written as

$$\mathrm{d}b/\mathrm{d}t = k_B(t)A = k_B t^{-h}A \quad (1)$$

$$\frac{\mathrm{d}C}{\mathrm{d}t} = k_C(t)A = k_C t^{-1}A \quad (2)$$

$$-\frac{\mathrm{d}A}{\mathrm{d}t} = \frac{\mathrm{d}B}{\mathrm{d}t} + \frac{\mathrm{d}C}{\mathrm{d}t} \quad (3)$$

where k_B and k_C are the initial rate coefficients (defined at the initial film thickness; Table 2) for the bonding and evaporation reactions, respectively, and $k_B(t)$ and $k_C(t)$ are the instantaneous rate coefficients, respectively. In the bonding reaction, eq 1, the functional form of the time dependence, h, has been observed to vary from 0.25 to 1.0, depending upon the lubricant chain flexibility and/or surface composition.[10,21] Evaporation is observed to proceed with a $t^{-1.0}$ time dependence. While the evaporation kinetics is not the focal point of this paper, its treatment is required for mass balance

(17) Frisch, M. J.; Trucks, G. W.; Head-Gordon, M.; Gill, P. M. W.; Wong, M. W.; Foresman, J. B.; Johnson, B. G.; Schlegel, H. B.; Robb, M. A.; Replogle, E. S.; Gomperts, R.; Andres, J. L.; Raghavachari, K.; Binkley, J. S.; Gonzalez, C.; Martin, R. L.; Fox, D. J.; Defrees, D. J.; Baker, J.; Stewart, J. J. P.; Pople, J. A. *Gaussian 92*, Revision C; Gaussian Inc.: Pittsburgh, PA, 1992.

(18) Pople, J. A.; Gordon, M. *J. Am. Chem. Soc.* **1967**, *17*, 4253.

(19) Pacansky, J.; Miller, M.; Hatton, W.; Liu, B.; Scheiner, A. *J. Am. Chem. Soc.* **1991**, *113*, 329. Pacansky, J.; Waltman, R. J.; Ellinger, Y. *J. Phys. Chem.* **1994**, *98*, 4787.

(20) Califano, S. *Vibrational States*; John Wiley & Sons: New York, 1976.

Table 1. SCF/3-21G Computed Vibrational Frequencies and Assignments for PFNPO

freq, cm^{-1}			Figure 1
	scaled 0.892	potential energy distribn and descripn	(top) assgnmt
1541.50	1375.0	C−F (CF_3) stretch	a
1540.47	1374.1	C−F (CF_3) stretch	a
1490.11	1329.2	C−F (CF_3) stretch	b
1483.59	1323.4	C−F (CF_3) stretch	b
1446.99	1290.7	C−F (CF_3) stretch + C−C stretch	b, c
1426.86	1272.8	C−O stretch + C−F (CF_2) stretch	c
1418.58	1265.4	C−F (CF_2) stretch	c
1382.32	1233.0	C−O stretch + C−F (CF_2) stretch	d
1379.22	1230.3	C−O stretch + C−F (CF_2) stretch	d
1372.67	1224.4	C−O stretch + C−F (CF_2) stretch	
1330.50	1186.8	C−O stretch + C−F (CF_2) stretch	e
1277.36	1139.4	C−F (CF_2) stretch	f
1132.91	1010.6	C−F (CF_3) stretch + C−C−F bend	g
858.59	765.9	F−C−O bend + C−C−O bend	h
698.82	623.4	F−C−F (CF_3) bend	
651.67	581.3	F−C−F (CF_3) bend + C−C−F bend	
596.95	532.5	C−C−O bend + C−C−F bend	

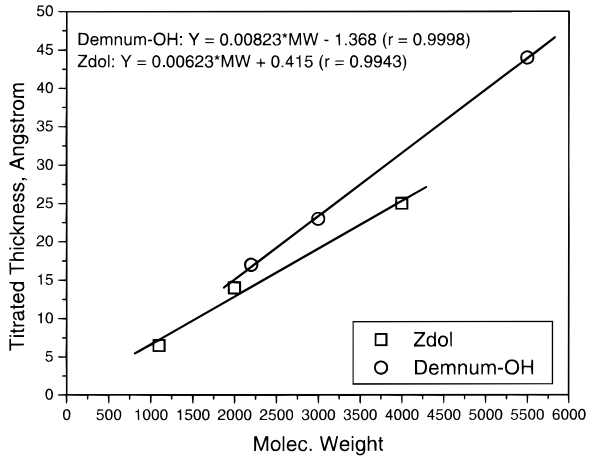

Figure 2. Titrated thicknesses for Demnum-OH and Zdol on CH_x amorphous hydrogenated carbon as a function of molecular weight.

(eq 3). Evaporation kinetics and the significance of the $t^{-1.0}$ time dependence is considered elsewhere.[22]

The solid lines accompanying the data points are obtained from the theoretical treatment discussed above, where we observe that a $t^{-0.5}$ time dependence in the bonding differential rate equation and a $t^{-1.0}$ time dependence in the evaporation differential rate equation, respectively, reproduce the experimental data, including the crossovers in the bonding curves (Figures 3 and 4 (middles)). Referring to Figure 3 (top), the fraction of mobile Demnum-OH decreases asymptotically to zero with increasing time and temperature. The depletion of mobile Demnum-OH from CH_x is quantitatively accounted for by increases in both the bonded fraction (Figure 3 (middle)) and the evaporated fraction (Figure 3 (bottom)). For Demnum-OH (MW 2200), the loss of mobile lubricant is dominated by the evaporation reaction, particularly at the higher temperatures, due to the relatively low molecular weight. The data presented in Figure 3 additionally serve to illustrate that

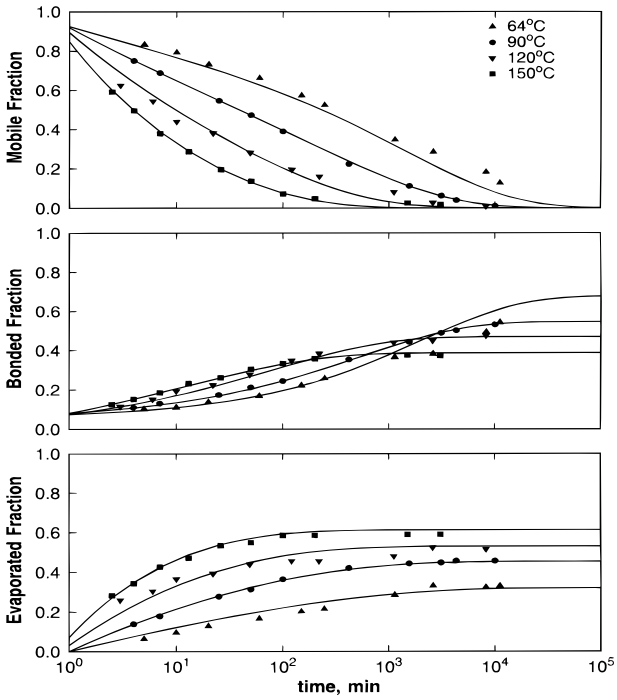

Figure 3. Changes in the (top) mobile, (middle) bonded, and (bottom) evaporated fractions of Demnum-OH (MW 2200) on CH_x as a function of time and temperature. All initial film thicknesses were 11.0 ± 0.5 Å. The solid lines that accompany the data points are obtained from the theoretical fits of eqs 1−3.

bonding and evaporation will continue to occur as long as mobile Demnum-OH is present on the disk, and the titrated thickness (Figure 2) is not exceeded in the bonding channel. On the basis of Figure 3, we conclude that evaporation from the bonded state does not occur over the range of temperatures and times investigated here.

The kinetic profiles for the changes in mobile, bonded, and evaporated Demnum-OH (MW 3000) on CH_x are presented in Figure 4. By increasing the molecular weight from 2200 to 3000, the competing evaporation reaction has been reduced significantly, Figure 4 (bottom). For example, at 64 °C, the asymptotic limit of the evaporated fraction is roughly $^1/_2$ of that previously observed for Demnum-OH (MW 2200). As a result, more lubricant is available for bonding as well as for main-

(21) Waltman, R. J.; Zhang, H.; Khurshudov, A.; Pocker, D.; Karplus, M.; York, B.; Xiao, Q.-F.; Zadoori, H.; Thiele, J.-U.; Tyndall, G. W. In *Proceedings of the Symposium on Interface Technology Towards 100 Gbit/in²*; Bhatia, C. S., Polycarpou, A. A., Menon, A. K., Eds.; American Society of Mechanical Engineers: New York, 1999 Trib-Vol. 9, p 53.

(22) Tyndall, G. W.; Waltman, R. J. *J. Phys. Chem.*, accepted for publication.

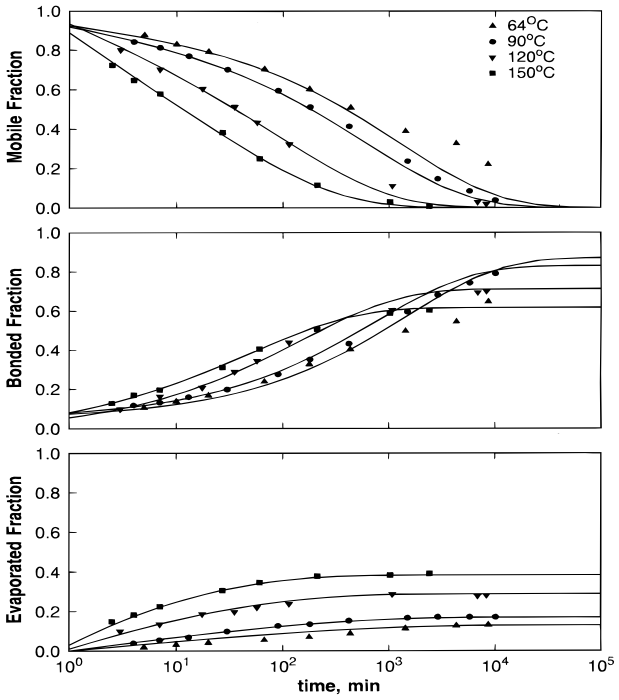

Figure 4. Changes in the (top) mobile, (middle) bonded, and (bottom) evaporated fractions of Demnum-OH (MW 3000) on CH_x as a function of time and temperature. All initial film thicknesses were 11.0 ± 0.5 Å. The solid lines that accompany the data points are obtained from the theoretical fits of eqs 1−3.

Table 2. Bonding and Evaporation Rate Coefficients for Demnum-OH as a Function of Molecular Weight and Temperature

	MW 2200		MW 3000	
temp, °C	k_B	k_C	k_B	k_C
64	0.00950	0.0630	0.0125	0.0238
90	0.0161	0.120	0.0173	0.0353
120	0.0338	0.191	0.0345	0.0790
150	0.0565	0.304	0.0515	0.135

taining surface coverage. The functional form of the kinetic time dependence for the bonding of Demnum-OH (MW 3000) is identical to Demnum-OH (MW 2200), $t^{-0.5}$.

(i) Ab Initio Data. The $t^{-0.5}$ time dependence observed for the bonding kinetics of Demnum-OH on CH_x, Figures 3 and 4, has been observed previously in *stiff* Zdol chains with a low C1:C2 (perfluoromethylene oxide:perfluoroethylene oxide) ratio. As the Zdol chain is increased in flexibility by increasing the C1:C2 ratio, the bonding time dependence is observed to follow $t^{-1.0}$. At moderate levels of chain flexibility, the time exponent *h* may equal to any number between 0.5 and 1.0.[10] Thus, chain flexibility, which reflects the degree of confinement of the adsorbed film, plays an important role in PFPE bonding. The chain flexibility determines the ability of PFPE lubricant to adopt conformations on the surface that are conducive to bonding, by allowing movement of the −OH end groups to find active sites on the carbon surface. Confinement of the chain either by the surface or by large barriers to internal rotation will affect bonding kinetics.

The focal point of these theoretical studies is to investigate the energetic barriers to internal rotation about the C−O and C−C bonds in the Demnum-OH main chain that govern chain flexibility, or lack thereof, and hence will impact the mobility of Demnum-OH on the amorphous carbon surface. In Demnum-OH, having the chemical repeat structure $-[CF_2CF_2CF_2O]-$, torsional potentials about C−C and C−O bonds will determine the flexibility of the main chain. Hence, we employ model structures for the Demnum-OH main chain that are computationally tractable and assess the barriers to internal rotation about the C−C and C−O bonds. We will use SCF, MP2 (Moeller−Plesset pertubation theory), and B3LYP[23] (density functional) methods at the 6-31G[d] basis set,[24] and the semiempirical PM3.[25] MP2 and B3LYP will allow for some corrections for electron correlation and will represent our most accurate calculations in this work. PM3 will also have parametrization accounting for some of the effects of electron correlation, and may provide a less expensive and reasonably accurate methodology for the evaluation of larger lubricant model structures. The semiempirical methods often have better mean absolute deviations from experiment compared to Hartree−Fock based methods.[26]

(a) CF_3CF_3. The calculated energy map for rotation about the C−C bond in perfluoroethane, PFE, presented in Figure 5, demonstrates that when the C−F bonds are staggered, local energy minima exist. Because all geometric parameters are optimized, these minima represent the stable conformers of PFE. Energy maxima occur in PFE when the C−F bonds are eclipsed (see Figure 5) and correspond to the barrier for internal rotation. From the data presented in Figure 5, rotation about the C−C bond is estimated to be ∼4 kcal/mol for both SCF and MP2 at 6-31G[d]. The same barrier is ∼3 kcal/mol at B3LYP, while PM3 provides a significantly lower ∼2 kcal/mol.

(b) CF_3OCF_3. The calculated minimum energy path for the internal rotation about the C−O bond in perfluorodimethyl ether, PFDME, is shown in Figure 6. The rotation of the C−O bond in PFDME is relatively unhindered, at ∼1 kcal/mol, separated by a double minimum with a smaller 0.3 kcal/mol barrier height (MP2). The optimized geometry for the global minimum has been discussed before.[27] The barrier maximum at the C1−O2−C6−F7 dihedral angle of −123° arises from the nonbonding close contact between C1 and F8 in the locally planar structure (C1−O2−C6−F8 dihedral angle of ∼−3°). The smaller barrier at the C1−O2−C6−F7 dihedral angle of −63° occurs from the interaction of the fluorine and oxygen lone pair of electrons. The conclusion to be drawn from these results is that the barrier for internal rotation about sterically unobstructed C−O bonds (such as in PFDME) will be significantly smaller than those for rotation about the C−C bonds in the perfluoroalkyl fragment. In this context, the torsional barrier to internal rotation for perfluoro(dimethoxymethane) or PFDMOM, $CF_3OCF_2OCF_3$, has been investigated by Schwartz et al.[28] PFDMOM is the simplest linear perfluoroether containing

(23) Becke, A. D. *J. Chem. Phys.* **1993**, *98*, 5648.
(24) Raghavachari, K.; Pople, J. A. *Int. J. Quantum Chem.* **1981**, *20*, 1067.
(25) Stewart, J. J. P. *J. Comput. Chem.* **1989**, *10*, 209, 221.
(26) Foresman, J. B.; Frisch, A. *Exploring Chemistry with Electronic Structure Methods;* Gaussian, Inc.: Pittsburgh, PA, 1996; Chapter 7.
(27) Pacansky, J.; Waltman, R. J. *J. Fluor. Chem.* **1997**, *82*, 79.

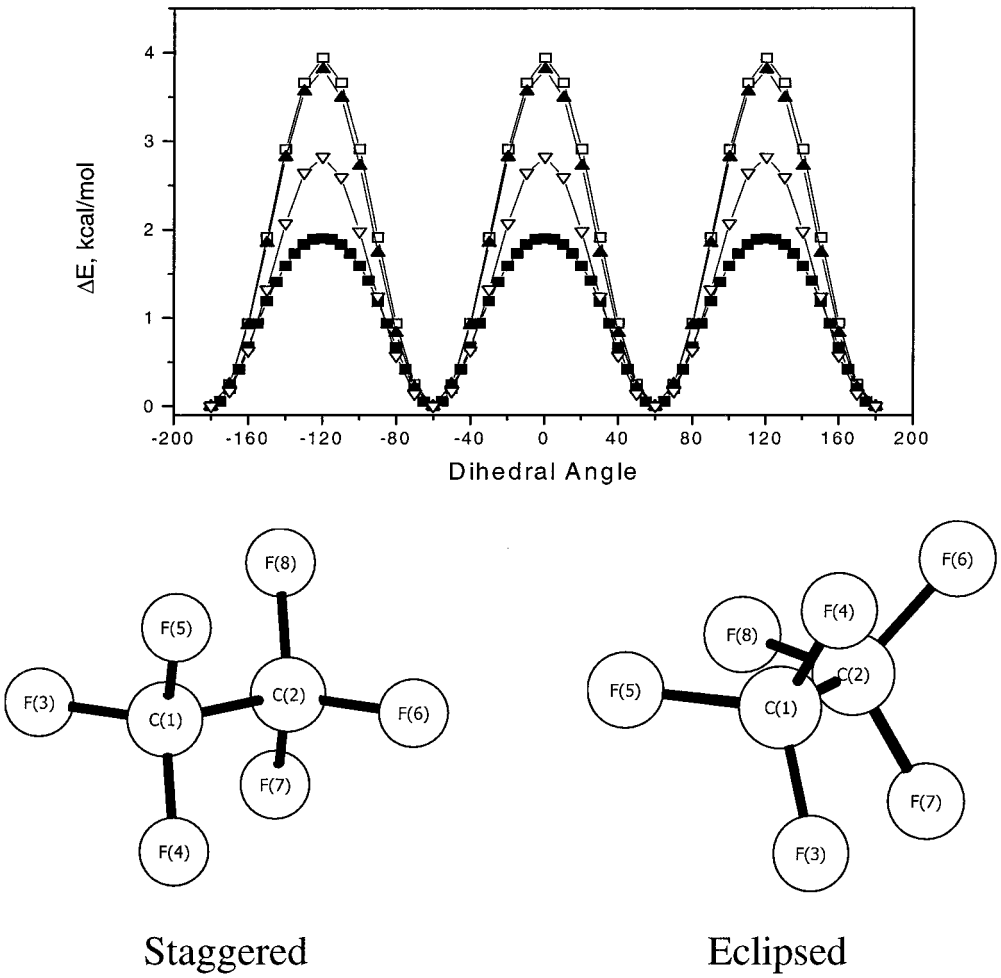

Figure 5. Torsional potential for the rotation of the C−C bond in perfluoroethane: (□) SCF/6-31G[d]; (▲) MP2/6-31G[d]; (▽) B3LYP/6-31G[d]; (■) PM3.

internal rotation about multiple C−O bonds. In their studies, a rotation about a single C−O bond in the "extended" (trans−trans) conformer produced a barrier of ∼1.3 kcal/mol at the 6-31G[d] basis set, similar to the results for PFDME discussed above. They have also produced a potential energy contour diagram for the simultaneous rotation of both C−O bonds, with the result that a relatively large number of conformers were accessible to PFDMOM at relatively small energy barriers.[28]

(c) $CF3OCF_2CF_2OCF_3$. The calculated minimum energy path for the internal rotation about the C−C bond in perfluorodimethoxyethane, PFDMOE, is shown in Figure 7. The computed barriers are similar to the simpler perfluoroethane considered previously in Figure 5; however, PFDMOE allows for the oxygen gauche effect[29] which puts the global minimum (except PM3) at ±60°, and not the extended trans structure at 180°, Figure 7. Figure 7 demonstrates that when the C−F and C−O bonds are staggered, local energy minima exist. Because all geometric parameters are optimized, these minima represent the stable conformers of PFE. Energy maxima occur in PFE when the C−F and C−O bonds are eclipsed (±120°, 0°, Figure 7) and correspond to the barrier for internal rotation. From the data presented in Figure 7, rotation about the C−C bond is estimated to be ∼4−5 kcal/mol for both SCF and MP2 at 6-31G-[d]. PM3 again provides a significantly lower ∼2 kcal/mol barrier.

In summary, the studies on the smaller models for the PFPE lubricant chain indicate that the computed barriers to internal rotation at SCF/6-31G[d] are in excellent agreement with the MP2 results and will suffice in the interpretation of the bonding kinetics. Thus, the computed barrier to internal rotation about C−C bonds is ∼4−5 kcal/mol (SCF, MP2) compared to ∼3 and 2 kcal/mol for B3LYP and PM3, respectively. For C−O rotations, ∼1−1.2 kcal/mol (SCF, MP2) is compared to ∼0.9 and 1.4 for B3LYP and PM3, respectively.

(d) $CF_3CF_2CF_2OCF_3$. $CF_3CF_2CF_2OCF_3$ (perfluoromethoxypropane, PFMOP) represents the smallest monomer unit for Demnum-OH, and the optimized geometry is shown in Figure 8 (−161°). The calculated minimum energy path for the internal rotation about the interior C−O (C6−O2) and C−C (C7−C6) bonds are shown in Figures 8 and 9. The barriers to internal rotation for the exterior C−O (C1−O2) and C−C (C7−C10) bonds are both quantitatively and qualitatively similar to Figures 6 and 5, respectively; thus, no reiteration is

(28) Stanton, C. L.; Schwartz, M. *J. Phys. Chem.* **1993**, *97*, 11221. Stanton, C. L.; Paige, H. L.; Schwartz, M. *J. Phys. Chem.* **1993**, *97*, 5901. Stanton, C. L.; Berry, R. J.; Schwartz, M. *J. Phys. Chem.* **1995**, *99*, 3473.

(29) Smith, G. D.; Jaffe, R. L.; Yoon, D. Y. *Macromolecules* **1995**, *28*, 5804.

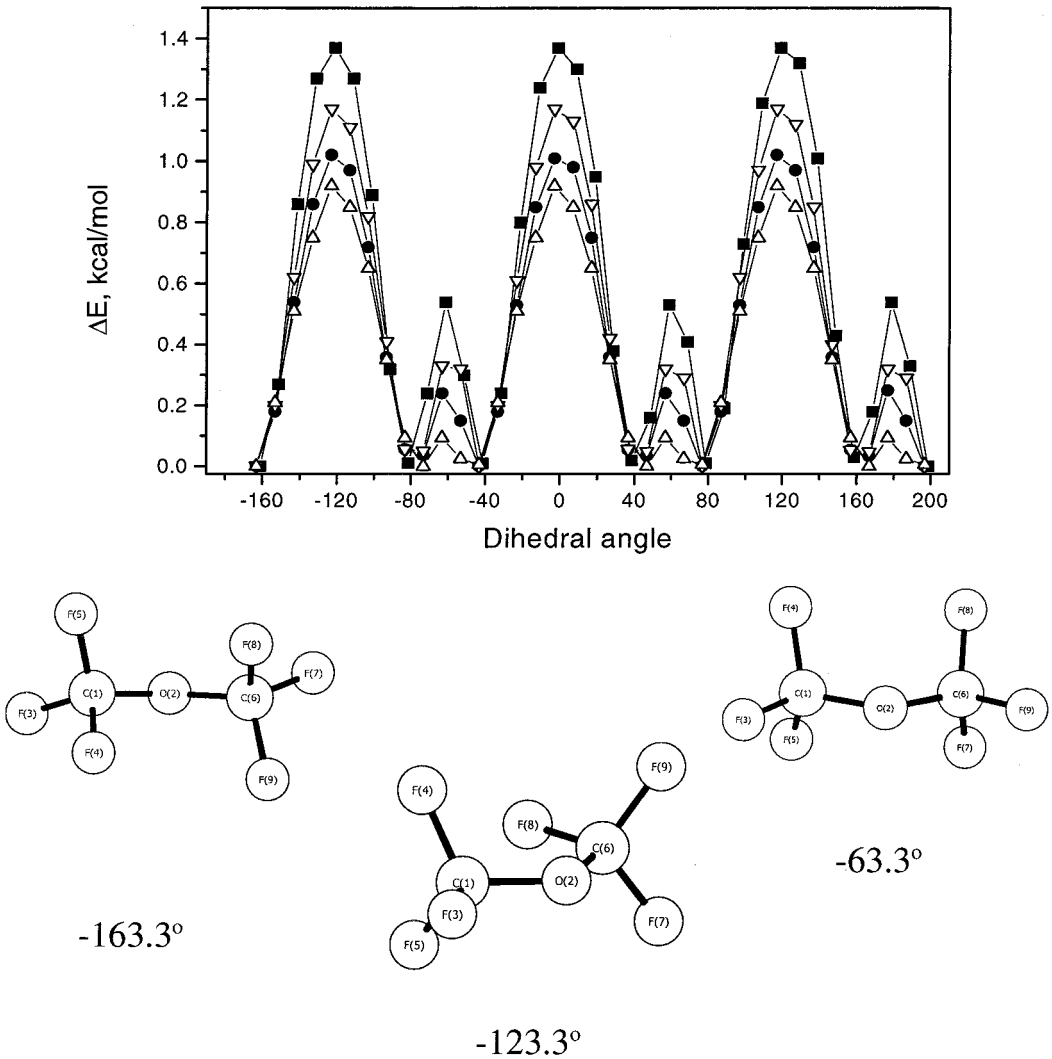

Figure 6. Torsional potential for the rotation of the C−O bond in perfluorodimethyl ether: (■) SCF/6-31G[d]; (▽) MP2/6-31G[d]; (●) B3LYP/6-31G[d]; (△) PM3.

given here. It is evident from Figure 8 that C−O rotations are severely hindered in the $-CF_2CF_2CF_2O-$ repeat unit with barrier maxima of 3 and 8 kcal/mol (SCF) at −71 and 0°, respectively. The barrier maximum at −71° arises from the eclipsed C1−F4/C6−F8 and C6−C7/C1−F5 bonds, with a nonbonding closest contact between F4 and F8 of 2.58 Å. The optimized geometry at 0° indicates a locally planar cis C7−C6−O2−C1 with steric interference between the eclipsed C1 and C7 groups. As before, PM3 apparently underestimates the large barrier predicted at 0°. Rotation about the interior C−C bond, Figure 9, exhibits the typical ∼4 kcal/mol (SCF) 3-fold torsional potential observed previously in $CF_3\cdots CF_3$ and $CF_3OCF_2\cdots CF_2OCF_3$. The barrier maximum arises when the C−F and C−C bonds at C7 are eclipsed with the C−F and C−O bonds at C6. Again, PM3 underestimates the barrier height by ∼2 kcal/mol.

(e) $CF_3CF_2CF_2OCF_2CF_2CF_3$. The studies above indicate that PM3 consistently underestimates the barriers to internal rotation of hindered C−C and C−O bonds in PFPE models. However, PM3 provides a computationally tractable methodology for evaluating larger systems such as perfluorodipropyl ether, PFDPE, presented in Figure 10. The torsional potentials for rotation about the interior C−O and C−C bonds indicate large barriers to internal rotation even at this level of theory. The conclusion to be drawn from these results is that rotation about the Demnum C−O bonds is significantly more hindered than Zdol $-CF_2O\cdots CF_2O-$ sectors. Thus, Demnum-OH chains are expected to be considerably stiffer than Zdol, consistent with the observed time dependence in the bonding kinetics discussed earlier. These studies indicate that conformational interconversion is significantly reduced as the number of CF_2 units between the ether oxygen atoms is increased, leading to greater confinement.

(ii) Molecular Mechanics Modeling: $F(CF_2CF_2CF_2O)$-CF_3. Molecular mechanics calculations were performed to simulate the conformation dependent variation in structure and energy of $CF_3CF_2CF_2OCF_3$, by investigating the *simultaneous* rotations of adjacent C−C and C−O bonds to generate three-dimensional energy−torsion plots.[30] The CVFF potential function was used for these calculations (using the Discover computational software[31] on IBM RISC 6000 computers). The analytic form of the CVFF potential function and the parameters used for the fluoroether models were previously described.[10] Three-dimensional potential energy contours

(30) Waltman, R. J.; Berry, R. J.; Pacansky, J. Previously unpublished data.

(31) *Insight II* (Version 2.1.0) and *Discover* (Version 2.8.0); Biosym Technologies, Inc.: San Diego, CA, 1993.

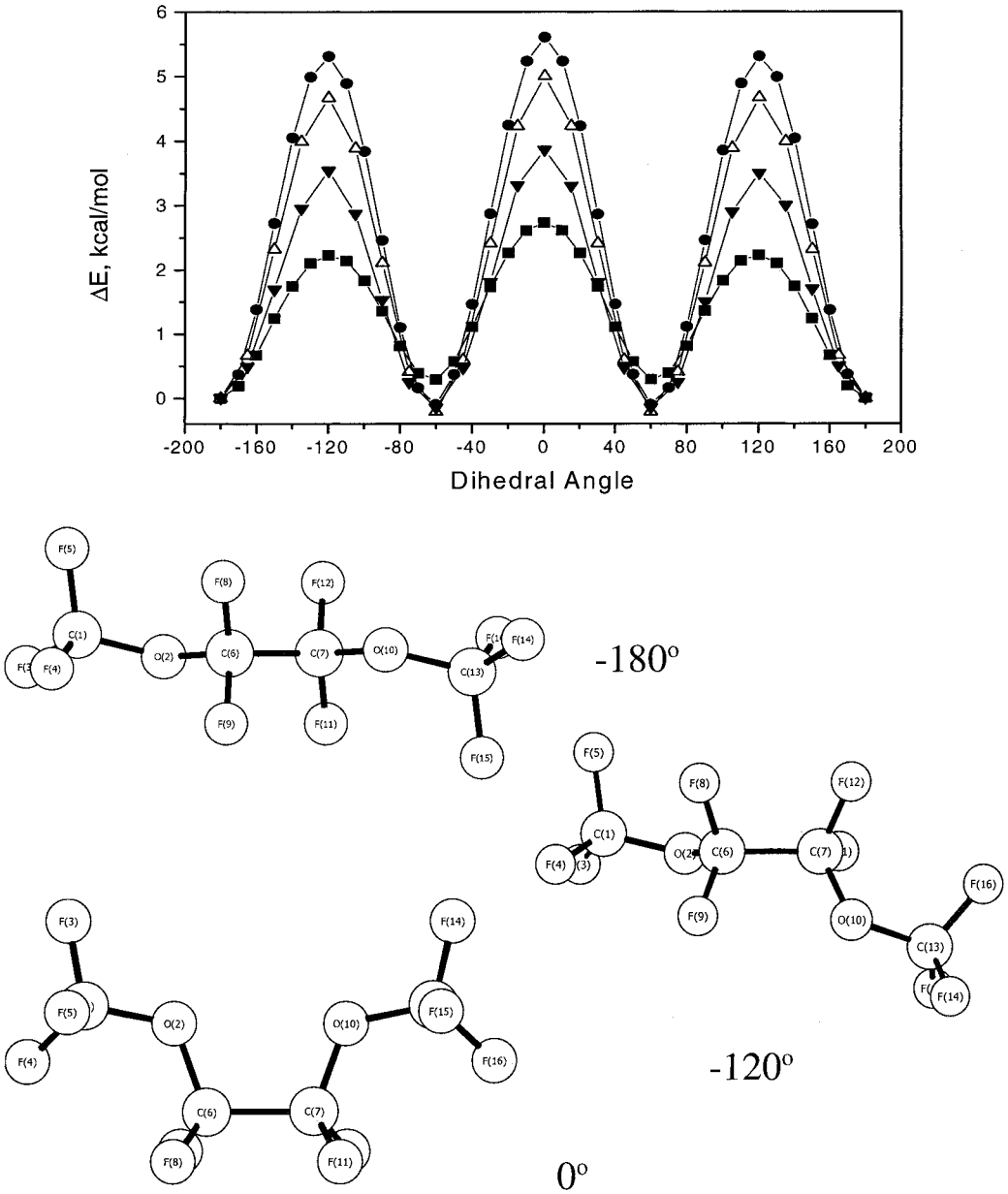

Figure 7. Torsional potential for the rotation of the C6−C7 bond: (●) SCF/6-31G[d]; (△) MP2/6-31G[d]; (▼) B3LYP/6-31G[d]; (■) PM3.

were calculated for $CF_3CF_2CF_2OCF_3$ as a function of the O2−C3−C4−C5 (*x*-axis) and C1−O2−C3−C4 (*y*-axis) dihedrals, Figure 11. Contour plots were generated by incrementing the dihedrals by 5° followed by a constrained minimization; i.e., the two dihedral angles were fixed while the remainder of the molecule was freely optimized, until the potential energies of the entire grid from −180 to +180° in both dihedrals were computed. The calculated energy contours as a function of C−O rotations for $CF_3CF_2CF_2OCF_3$ are presented in Figure 11 along with several of the key conformations that define the energy contours. The CVFF force field predicts a global minimum for the conformer B, defined by C1−O2−C3−C4 and O2−C3−C4−C5 dihedral angles of ⟨179°,168°⟩. These results are consistent with ab initio calculations as summarized in Table 3. Two additional low-energy configurations are identified on the contour map, brought about by the rotation of the C3−C4 bond. Conformer A, locacted at ⟨60°,168°⟩, is attained by a ∼120° rotation of the O2−C3−C4−C5 dihedral, and conformer B, located at ⟨−60°,170°⟩, is attained by an additional ∼120° rotation of the O2−C3−C4−C5 dihedral. While the energies of these configurations are nearly the same, interconversion requires surpassing a barrier of ∼3−4 kcal/mol and is not expected to readily occur at room temperature. The O2−C3−C4−C5 dihedral of ⟨0°,0°⟩ defines the transition state with a large barrier of ∼30 kcal/mol. The transition state arises from the steric inteference between the fluorine atoms of the perfluoromethyl groups at C1 and C5. The energy contour map provides the additional information that low-energy conformers are relatively confined and interconversion at room temperature is quite unlikely; i.e., the Demnum chains are expected to be quite "stiff" based upon this model. The geometries of these four conformers were additionally optimized at the SCF/6-31G[d] level of theory to corroborate the molecular mechanics results.[30] As shown in Table 3, the CVFF prediction of three low-energy conformers (ΔE = ∼0.4 kcal/mol) is consistent with the ab initio calculations,

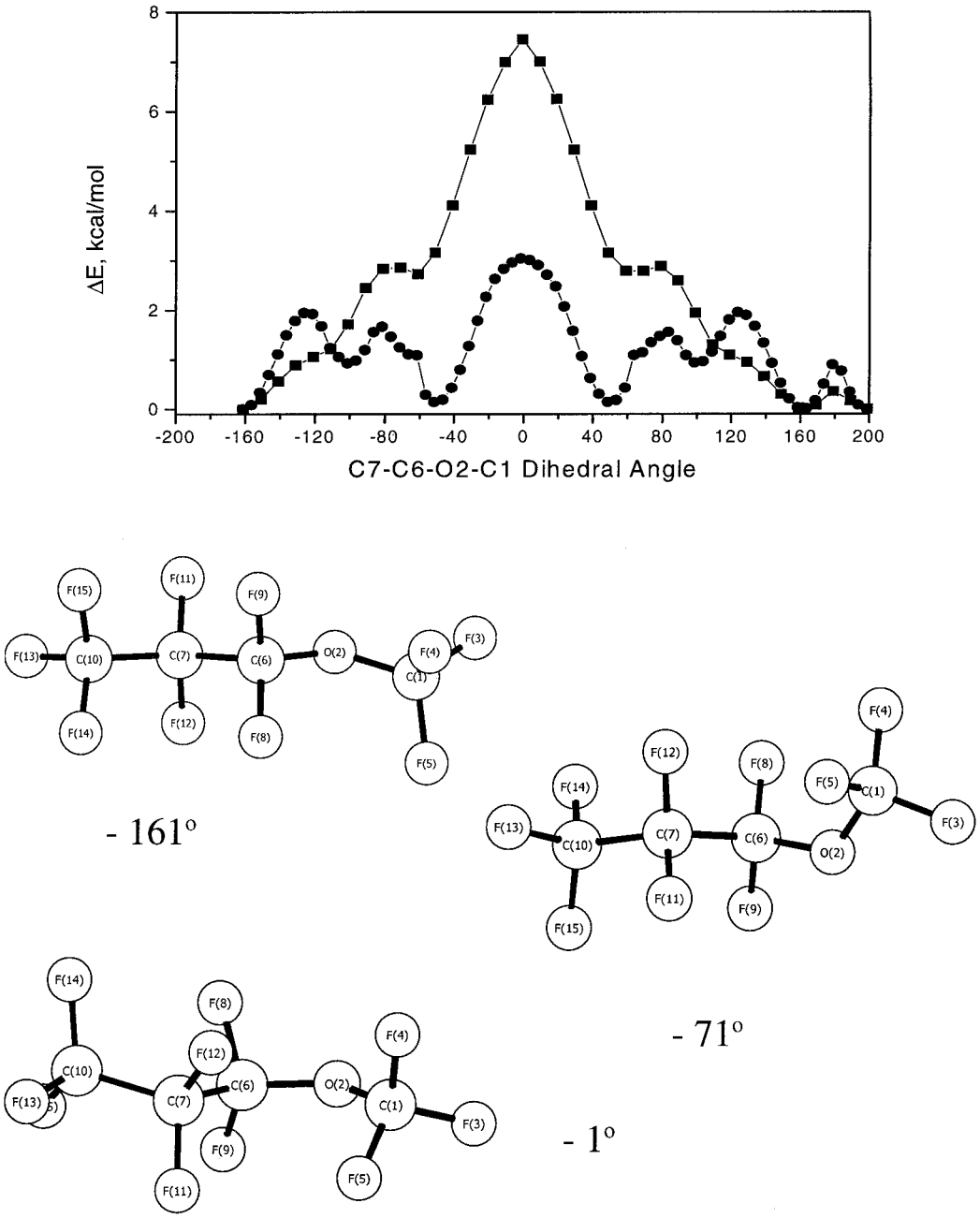

Figure 8. Torsional potential for the rotation of the C6−O2 bond: (■) SCF/6-31G[d]; (●) PM3.

$\Delta E = \sim 0.1$ kcal/mol. Thus, we conclude that the CVFF force field provides a reasonable representation of the energy contour plot.

The three-dimensional energy contour plots presented in Figure 11 along with the ab initio torsional potentials shown previously in Figures 8−10 provide insight into the relative flexibility of the Demnum-OH chain. The major conclusions that can be drawn from these computational studies are as follow: (a) rotations about C−C bonds are ∼4 kcal/mol and relatively difficult at room temperature; (b) rotations about the C−O bond in $CF_3CF_2CF_2OCF_3$ are comparatively more difficult than C−O rotations in CF_3OCF_3 or $CF_3OCF_2OCF_3$ [28] as a result of the higher energy barriers due to steric effects. The implications of these results to the Demnum-OH lubricant are straightforward. Since rotations about the C−O bond in the sterically hindered $-CF_2-CF_2CF_2OCF_2-$ monomer units are much more difficult than rotations about the C−O bonds in the sterically unobstructed $-OCF_2OCF_2-$ units, the Demnum-OH backbone will be stiffer than (flexible) Zdol and, consequently, exhibit the $k(t) \alpha t^{-0.50}$ bonding kinetics typical of stiff chains, just as we have observed previously for inflexible Zdol with low C1:C2 monomer units ratio.[10] We conclude that chain flexibility can be a significant determinant in the bonding kinetics of perfluoroalkylpolyether lubricants. A lack of chain flexibility decreases the configurational entropy of the lubricant boundary layer, serving to increase the confinement of the lubricant in the boundary layer. The origin for confinement is a decreased conformational accessibility attributed to relatively larger barriers to internal rotation.

One final comment regarding chain flexibility in PFPEs is presented here. The chain stiffness decreases with the decreasing number of carbons between the

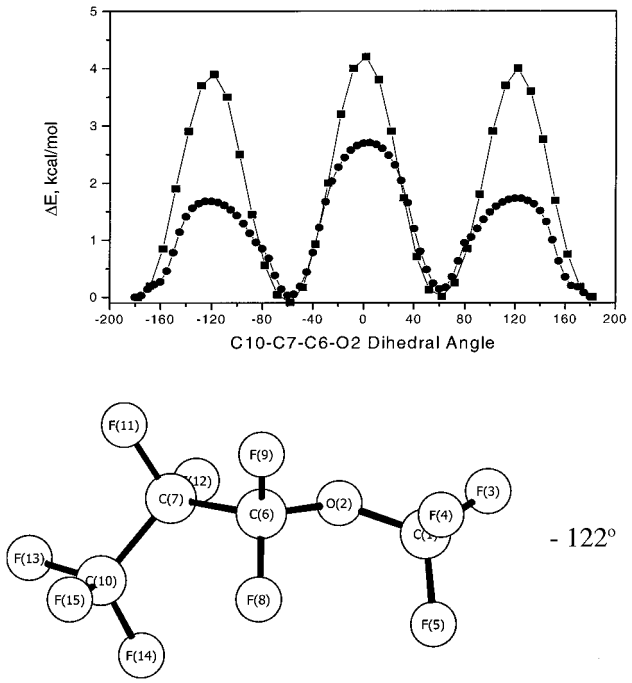

Figure 9. Torsional potential for the rotation of the C6−C7 bond: (■) SCF/6-31G[d]; (●) PM3.

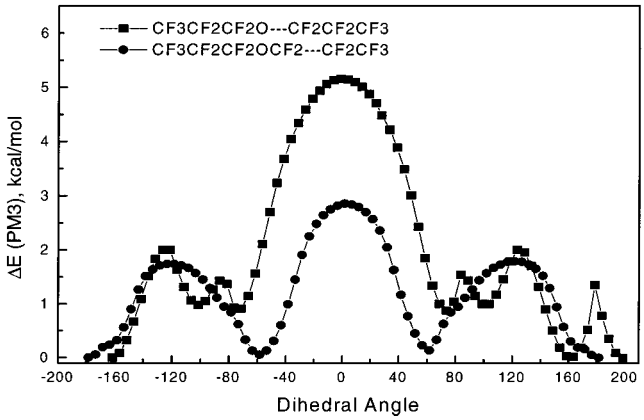

Figure 10. PM3 torsional potential for the rotation of C−O and C−C bonds.

ether oxygens, and C−C rotations in $-OCF_2CF_2O-$ structures (present in Zdols) exhibit an oxygen gauche effect,[29] Figure 7. The oxygen gauche effect may induce "kinks" in a linear chain. Consequently, the adsorbed film structure in a monolayer can be considerably different for Zdols and Demnums. In Figure 2, the titrated thickness in a monolayer was presented for Zdols and Demnum-OHs as a function of molecular weight. The differences in the slopes for the Demnum-OH and Zdol titration plots may provide an indication for differences in the adsorbed film structure. It is well-established that the adsorption of macromolecules on surfaces leads to alternate sequences of adsorbed segments, called "trains," and dangling segments, called "loops." Trains are the planar two-dimensional segments adsorbed to the surface, and loops are the three-dimensional segments located away from the surface. Larger adsorption energies favor the formation of trains, resulting in molecules that are closer to the surface.[12,13] However, the flatter the macromolecule, the larger the decrease in entropy that opposes adsorption.[7] The

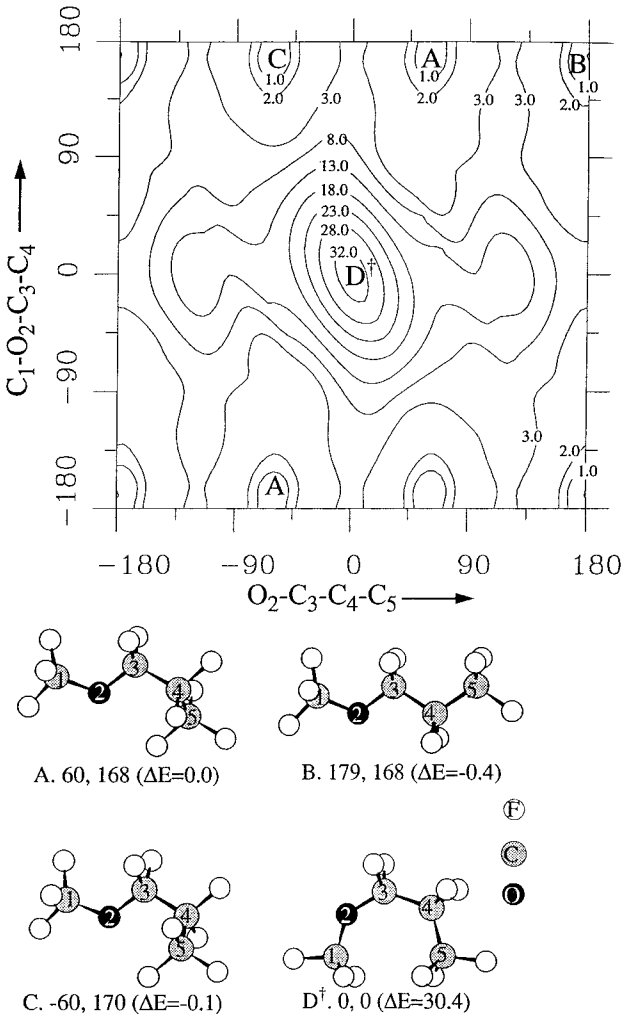

Figure 11. Energy contours for PFNPO as a function of the C−O−C−C and O−C−C−C dihedral angles. The relative energy, in kilocalories per mole, for each contour line is specified in the figure. The global minimum occurs for conformer B. Conformer D is a transition state identified by "‡" in the plot.

relative distribution of trains and loops in the boundary layer has been used to explain why the thickness of the adsorbed layer of macromolecules exceeds that of a monolayer.[12] The titration data shown in Figure 2 indicate that, at equivalent molecular weights, the effective thickness of the titrated Demnum-OH layer is greater than that of Zdol. In the molecular weight range examined, the maximum bonded thickness, A_m, fits the empirical relationship

$$A_m = KM^a \qquad (4)$$

where K and a are constants and M is the molecular weight. The conformation of the adsorbed chain may be estimated by the magnitude of a.[32] For example, when a = zero, the maximum adsorption thickness is independent of molecular weight, indicating that the configuration of the macromolecule on the surface is planar, i.e., adsorption by train. When a = one, the macromolecule on the surface has been interpreted as being held by a single segment or train. Between these two values for a, the loop-to-train ratio increases with increasing

(32) Perkel, R.; Ullman, R. *J. Polym. Sci.* **1961**, *54*, 127.

Table 3. Comparison of the Relative Conformational Energy (kcal/mol) vs Dihedral Angle for Perfluoro(methyl propyl ether)[49]

	rel energy, kcal/mol			
method	conformation A (Figure 9)	conformation B (Figure 9)	conformation C (Figure 9)	conformation D (Figure 9)
CVFF	0.0	−0.4	−0.1	30.4
SCF/6-31G[d]	0.0	0.1	0.1	24.6

a. A log−log plot of the data contained in Figure 2 provides the slopes (a) for all of the lines, tabulated

	plots of eq 4	
	A_m vs $M^{1.0}$	ln A_m vs ln $M^{1.0}$
K		
Demnum-OH	0.00823	0.00557
Zdol	0.00623	0.00477
a		
Demnum-OH	1.000	1.042
Zdol	1.000	1.038
correlation coeff		
Demnum-OH	0.9998	0.9998
Zdol	0.9943	0.9925

above, which are ∼1 for the titration of Zdol and Demnum-OH on CH_x, and justifies the linear plot. For the titration data, we interpret $a \sim 1$ as meaning that the bonded lubricant is anchored to the carbon surface by one hydroxyl end group for Demnum-OH and two hydroxyl end groups for Zdol. An $a \sim 1$ also suggests that the adsorbed film structure is not dominated by trains. Thus, the titrated thickness scales linearly with molecular weight in the molecular weight regime indicated and is indicative that the adsorption of lubricant on CH_x results in a boundary film structure that contains appreciable loops. The constant *K*, which is the slope of the lines in Figure 2, is also observed to increase from Zdol to Demnum-OH. We interpret the magnitude of *K* as indicative of the size of the loops in the adsorbed film. Since *K* is larger for Demnum-OH than for Zdol, Demnum-OH contains larger loops.

Concluding Remarks

The focal point of these studies was to provide a structure−property correlation of lubricant mobility as defined by bonding kinetics on amorphous hydrogenated carbon, CH_x. Thus, the bonding kinetics of Demnum-OH, having the $-[CF_2CF_2CF_2O]-$ monomer repeat unit, was compared to Zdol, having the $-[CF_2O]$-///-$[CF_2CF_2O]-$ monomer repeat units. The kinetics of the Demnum-OH bonding to a CH_x surface was investigated as a function of molecular weight, temperature, and time. The bonding rate constant in all cases was found to be time dependent, $k(t) = k_o t^{-0.5}$. The $t^{-0.5}$ time dependent bonding rate was postulated to result when bonding occurs from lubricant chains that are relatively inflexible and confined on a surface. The intrinsic mobility of Demnum-OH was interpreted by computational modeling using ab initio and molecular mechanics methods. Information on the flexibility of the Demnum-OH backbone, $-[CF_2CF_2CF_2O]-$, was obtained by calculation of the energetic barriers to internal rotation about C−O and C−C bonds. Ab initio calculations indicated a comparatively large energetic barrier to internal rotation about the C−O bond in Demnum chains, ∼6 kcal/mol, compared to Zdol models having barriers to internal rotation as small as ∼1 kcal/mol. Barriers about C−C rotations in Demnum and Zdol chains were ∼4 kcal/mol. Thus, Demnum chains are much stiffer than Zdol chains, consistent with the experimental bonding data. These results demonstrate that the configurational entropy of lubricants in the boundary layer is an important determinant of lubricant mobility.

Acknowledgment. R.J.W. gratefully acknowledges many fruitful discussions with G. W. Tyndall, J. Pacansky, and B. Lengsfield (IBM Almaden Research Center) and C. M. Mate (IBM Almaden Research Center) for the samples of Demnum-SA2 and -SA3 used in this work.

CM0001410